

Original Article

***In utero* and lactational 2,3,7,8-tetrachlorodibenzo-*p*-dioxin (TCDD) exposure exacerbates urinary dysfunction in hormone-treated C57BL/6J mice through a non-malignant mechanism involving proteomic changes in the prostate that differ from those elicited by testosterone and estradiol**

Anne E Turco^{1,4*}, Samuel Thomas^{1,4,6*}, LaTasha K Crawford², Weiping Tang³, Richard E Peterson^{1,3}, Lingjun Li^{1,3,5}, William A Ricke^{1,3,4,6}, Chad M Vezina^{1,2,4,6}

¹Molecular and Environmental Toxicology Center, ²School of Veterinary Medicine, ³School of Pharmacy, ⁴George M. O'Brien Center of Research Excellence, Departments of ⁵Chemistry, ⁶Urology, University of Wisconsin-Madison, Madison, WI, USA. *Equal contributors.

Received December 20, 2019; Accepted January 7, 2020; Epub February 25, 2020; Published February 28, 2020

Abstract: A recent study directed new focus on the fetal and neonatal environment as a risk factor for urinary dysfunction in aging males. Male mice were exposed *in utero* and via lactation (IUL) to the persistent environmental contaminant 2,3,7,8-tetrachlorodibenzo-*p*-dioxin (TCDD) and then administered slow-release, subcutaneous implants of testosterone and estradiol (T+E2) as adults to mimic the hormonal environment of aging men. IUL TCDD exposure worsened T+E2-induced voiding dysfunction. Mice in the previous study were genetically prone to prostatic neoplasia and it was therefore unclear whether TCDD exacerbates voiding dysfunction through a malignant or non-malignant mechanism. We demonstrate here that IUL TCDD exposure acts via a non-malignant mechanism to exacerbate T+E2-mediated male mouse voiding dysfunction characterized by a progressive increase in spontaneous void spotting. We deployed a proteomic approach to narrow the possible mechanisms. We specifically tested whether IUL TCDD exacerbates urinary dysfunction by acting through the same prostatic signaling pathways as T+E2. The prostatic protein signature of TCDD/T+E2-exposed mice differed from that of mice exposed to T+E2 alone, indicating that the mechanism of action of TCDD differs from that of T+E2. We identified 3641 prostatic proteins in total and determined that IUL TCDD exposure significantly changed the abundance of 102 proteins linked to diverse molecular and physiological processes. We shed new light on the mechanism of IUL TCDD-mediated voiding dysfunction by demonstrating that the mechanism is independent of tumorigenesis and involves molecular pathways distinct from those affected by T+E2.

Keywords: 2,3,7,8-tetrachlorodibenzo-*p*-dioxin, TCDD, prostate, proteomics, urinary dysfunction

Introduction

Urinary voiding dysfunction can lead to a constellation of lower urinary tract symptoms (LUTS) such as increased urgency and frequency (especially at night) and pain [1]. LUTS occur at a high rate in aging men [2], are expensive [3], and diminish quality of life [4]. The pathogenesis of voiding dysfunction in aging men is now considered complex and can include nodular benign prostatic hyperplasia (BPH), prostatic and/or bladder fibrosis, enhanced prostatic

smooth muscle contractility and neural dysfunction, among other mechanisms [5, 6]. Many of these pathologies cause voiding dysfunction and symptoms by obstructing urine passage through the prostatic urethra.

We developed a mouse model of spontaneous urinary voiding dysfunction characterized by an obstructive voiding pattern to identify new mechanisms and disease confounders. Adult male mice are treated with slow-release, subcutaneous implants of testosterone and estradiol

Developmental dioxin impacts adult urinary function

(T+E2) to mimic hormonal changes occurring in aging men [7]. T+E2 treatment drives mouse prostatic proliferation and enlargement, prostatic smooth muscle thickening, and urinary dysfunction characterized by more frequent small volume urine deposits, retention of urine in the bladder, increased bladder wet weight (hypertrophy), and progression towards hydro-nephrosis and renal impairment [8-10]. T+E2-induced mouse pathologies parallel those observed in men with prostate related voiding dysfunction [11].

We used T+E2-treated mice to screen for risk modifiers of male urinary voiding dysfunction [10, 12]. A paradigm-shifting outcome was the recognition that adult male voiding function is not only shaped by the adult environment, but also by the fetal and neonatal environments. For example, *in utero* and lactational exposure to the persistent environmental contaminant 2,3,7,8-tetrochlorodibenzo-*p*-dioxin (TCDD) worsened T+E2-induced urinary dysfunction in male Tg(CMV-*cre*);*Nkx3-1*(+/-);*Pten*(fl/+) mice that are genetically prone to prostatic neoplasia [12]. Therefore, it was unclear whether TCDD exacerbates voiding dysfunction through a malignant or non-malignant mechanism. Resolving the mechanism is important because there is precedence that TCDD can accelerate and increase aggressiveness of prostate cancer in susceptible mice [13, 14] and because prostate cancer in mice and men can cause urinary voiding dysfunction [15].

The present study involved wild type mice (C57BL/6J) that are not genetically prone to prostate cancer and that were divided into four experimental groups: (1) unexposed control mice (control), (2) mice exposed *in utero* and via lactation to TCDD only and not to T+E2 (TCDD alone), (3) mice exposed to T+E2 beginning at six weeks of age but not TCDD (T+E2 alone), and (4) mice exposed to TCDD and T+E2 (TCDD/T+E2). We used the void spot assay to test the hypothesis that voiding dysfunction is worse in TCDD/T+E2 than T+E2 alone mice. While deposited urine spots did not differ between TCDD alone and control mice, TCDD/T+E2 mice deposited more urine spots than T+E2 alone mice. This outcome is important because it suggests that early life TCDD exposure exacerbates T+E2-mediated voiding dysfunction through a mechanism independent of tumorigenesis.

Early-life TCDD exposure could exacerbate urinary voiding dysfunction by further changing T+E2-affected genes and signaling pathways or by acting through distinct, but physiologically complementary pathways. We leveraged results from a previous study in which we identified a T+E2 prostatic protein signature (33 proteins significantly altered in abundance by T+E2 alone compared to control). We tested whether TCDD/T+E2 exposure changes the abundance of these 33 proteins beyond the changes elicited by T+E2 alone [16]. TCDD/T+E2 surprisingly had little additional impact, significantly changing the abundance of just one of the 33 proteins. Instead, TCDD/T+E2 changed the abundance of a distinct group of proteins vs T+E2 alone, including proteins linked to smooth muscle and neural function and development, fibrosis, and inflammation. We shed new light on the mechanism of IUL TCDD-mediated voiding dysfunction by demonstrating that TCDD/T+E2 acts independent of a tumorigenic mechanism and through molecular pathways distinct from those affected by T+E2 alone.

Experimental section

Mouse treatment

All mouse protocols and procedures were approved by the University of Wisconsin Animal Care and Use Committee and performed following the National Institutes of Health Guide for the Care and Use of Laboratory Animals. All mice were C57BL/6J and purchased from Jackson Laboratories (stock number 0.000664, Bar Harbor, ME). Mice were housed in Innovive® HDPE plastic microisolator cages in a room maintained on a 12-h light and dark cycle with ambient temperature of 20.5 ± 1°C and relative humidity of 30-70%. Mice were fed a 5015 Diet (PMI Nutrition International, Brentwood, MO) from conception through weaning (P21) and a 8604 Teklad Rodent Diet after weaning (Harlan Laboratories, Madison, WI). Feed and water were available *ad libitum* and cages contained corncob bedding. All mice were euthanized by isoflurane overdose and cervical dislocation. Male mice were generated by time-mating males and females overnight. The morning of definitive copulatory plug identification was considered E0.5. Females with a body weight increase of 4 g (indicating pregnancy) were given either a single dose of TCDD

Developmental dioxin impacts adult urinary function

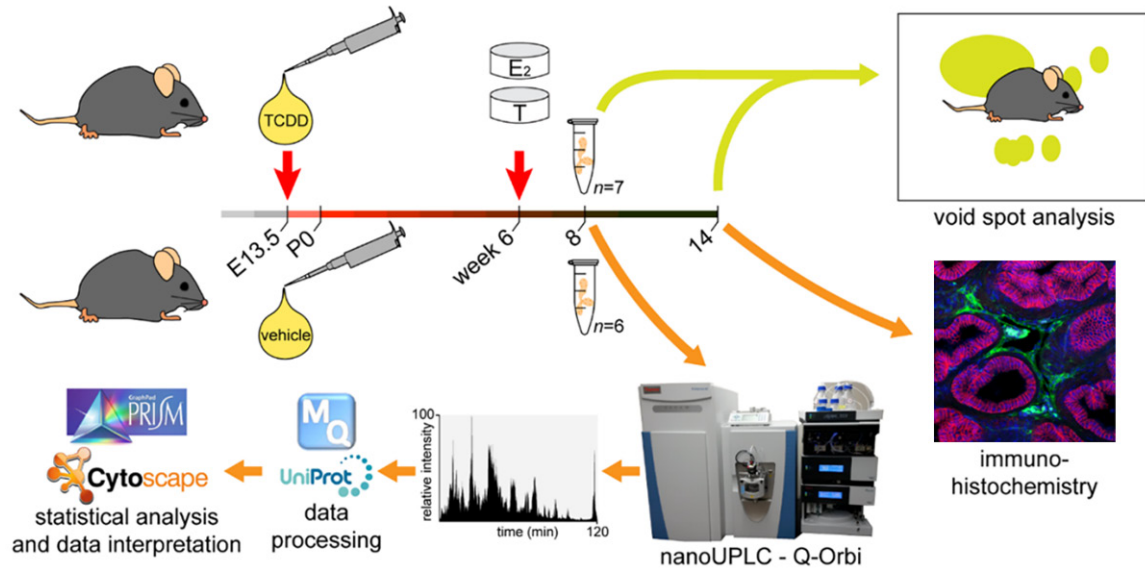


Figure 1. Experimental design. Male mice were exposed *in utero* and via lactation to TCDD (1 µg/kg oral maternal dose) or vehicle (5 mL/kg corn oil). Mice were aged to six weeks and given a sham surgery or implanted with hormone pellets consisting of 25 mg testosterone, 2.5 mg estradiol, and 22.5 mg cholesterol. Void spot assays were conducted two and eight weeks after implantation surgery to test for progressive urinary dysfunction. Prostate tissue was collected two and eight weeks post-implantation surgery for proteomic analysis or for staining.

(1 µg/kg, *per os*) or corn oil (vehicle) (5 mL/kg) at E13.5. TCDD (98% purity) was purchased from Cambridge Isotope Laboratories (Andover, MA). The TCDD dose matches that of a previous reference study [12]. Based on the established whole body elimination half-life of TCDD in C57Bl/6J mice, the TCDD dosing paradigm used in this study results in continuous TCDD exposure from the fetal period through weaning [17]. Male offspring were aged to six weeks, anesthetized and an implantation surgery was performed either as a sham surgery or to subcutaneously deliver a slow-release 25 mg testosterone implant (Steraloids, Newport Rhode Island) and a 2.5 mg 17β-estradiol + 22.5 mg cholesterol implant (Sigma Aldrich, St. Louis, MO) as previously described [8]. Experimental mice underwent contrast-enhanced ultrasound (following NIH reduce and reuse policy) before euthanasia. As a result, each mouse had Tamsulosin (10 µg/kg) in their system for 15 minutes prior to euthanasia. Graphical abstract illustrates the sequential methods.

Void spot assay (VSA)

Void spot assays (VSA) were conducted as described [18] two weeks post implantation

surgery on 23 control, 17 TCDD alone, 19 T+E2 alone, and 16 TCDD/T+E2 mice. VSAs were also conducted eight weeks post implantation surgery on 11 control, six TCDD alone, 14 T+E2 alone, and seven TCDD/T+E2 mice. Briefly, male experimental mice were housed for four h in clean cages lined with three mm Whatman filter paper (Fisher Scientific No. 057163W). Assays were conducted in a lighted room in the same quiet location and time of day. Food was provided during the assay but not water. Filter papers were imaged using ultraviolet light on a transilluminator and analyzed using Void Whizzard Software [18].

Mass spectrometry

Prostates (half of the anterior, ventral, and dorsolateral prostate lobes) were collected two weeks after implantation surgery from seven male TCDD/T+E2 mice and six T+E2 alone mice, frozen on dry ice, and stored at -80°C until further processing (Figure 1). Each mouse was analyzed as a single biological unit. Prostates were digested and further processed into peptides using a modified surfactant-aided technique as previously described [19]. Briefly, frozen prostates were thawed and homogenized in a solution containing sodium

Developmental dioxin impacts adult urinary function

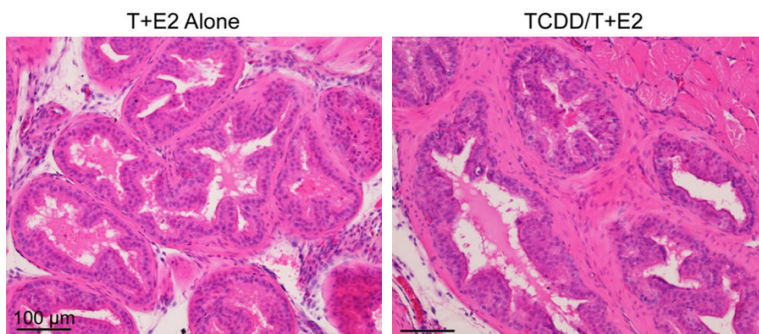


Figure 2. The effect of TCDD/T+E2 exposure compared to T+E2 alone in C57Bl6/J mice. Mouse prostate tissue sections (10 μm) from TCDD/T+E2 and T+E2 alone were stained using hematoxylin and eosin and examined by a board-certified veterinary pathologist. There was no evidence of high grade neoplasia or invasive carcinoma in either group. Images depict proximal dorsal prostate after two weeks of T+E2. Scale bar represents 100 μm . ($n = 3$).

dodecyl sulfate, deoxycholic acid, and a reducing agent in an ammonium bicarbonate buffer (Sigma, St. Louis, MO). Aliquots of homogenate were added to pre-passivated 30 kDa centrifugal filter units (Millipore, Burlington, MA) for urea buffer exchange and alkylation, followed by 18 h digestion with sequencing-grade trypsin (Promega, Madison, WI), and final collection of peptides. Peptides were desalted via C18 OMIX pipette tips (Agilent, Santa Clara, CA) before BCA assay (Thermo, Waltham, MA). Lyophilized peptides were stored at -80°C until analysis.

Mass spectrometry-based, label-free proteomics with relative quantification was used to assess prostatic protein abundance differences between TCDD/T+E2 and T+E2 mice. Prostatic peptides were analyzed on a Thermo Dionex nanoLC system coupled to a Thermo Q Exactive HF mass spectrometer. A C18 column was fabricated in-house with an integrated electrospray ionization emitter (75.1 $\mu\text{m}\times 150$ mm, BEH 1.7 μm , 130 \AA). Samples were kept at 4°C in the autosampler. Mobile phase A was 0.1% formic acid in H_2O and mobile phase B was 0.1% formic acid in acetonitrile (Fisher, Hampton, NH). The flow rate was 0.3 $\mu\text{L}/\text{min}$. The nanoLC gradient was as follows: 0-16 min 3% B, 16-106 min 3-30% B (linear), 106-106.5 min 30-75% B (linear), 106.5-116 min 75% B, 116-116.5 min 75-95% B (linear), 116.5-126 min 95% B, 126-126.5 min 95-3% B (linear), 126.5-141 min 3% B. We previously identified 66 peptide ions representing 33 proteins (2 peptides per protein) with abundance differ-

ences in urine and prostates of T+E2 alone compared to control mice (Table S1; [16]). We describe these proteins collectively as the T+E2 prostatic protein signature. The T+E2 prostatic protein signature includes proteins involved in inflammation, oxidative stress defense, and other processes. Global proteomics data were collected, with preference to peptide ions belonging to the T+E2 prostatic protein signature (as an inclusion list). Mass spectra were scanned from m/z 300-1,500 at a resolving power of 60K (at

m/z 200) and an S-lens radio frequency of 30. Parent masses were isolated in the quadrupole with an isolation window of 1.4 m/z and fragmented with higher-energy collisional dissociation with a normalized collision energy of 30 eV. MS/MS scans were detected in the Orbitrap using the rapid scan rate, a dynamic exclusion time of 45 s, and a resolution of 15K (at m/z 200). Automatic gain control targets were 1×10^6 for MS and 1×10^5 for MS/MS acquisitions. Maximum injection times were 100 ms for MS and 110 ms for MS/MS.

Immunostaining

Whole lower urinary tracts from three male TCDD/T+E2 mice and three T+E2 alone mice were collected two weeks after T+E2 implantation for Harris hematoxylin and eosin Y staining and evaluated by a board-certified veterinary pathologist for the presence of neoplasia (Figure 2). The dorsal prostate was imaged in representative regions.

Whole lower urinary tracts from three TCDD/T+E2 mice and three T+E2 alone mice were collected two weeks after implantation surgery and tissue sections were immunostained for ryanodine receptor 1 according to a previously described protocol [20, 21] (Figure 1). The dorsal prostate was imaged in representative regions. Briefly, lower urinary tracts were fixed in a sagittal orientation in 10% formalin overnight, dehydrated in graded alcohols, embedded in paraffin wax, and cut into five-micron sections. Tissue sections were dewaxed,

Developmental dioxin impacts adult urinary function

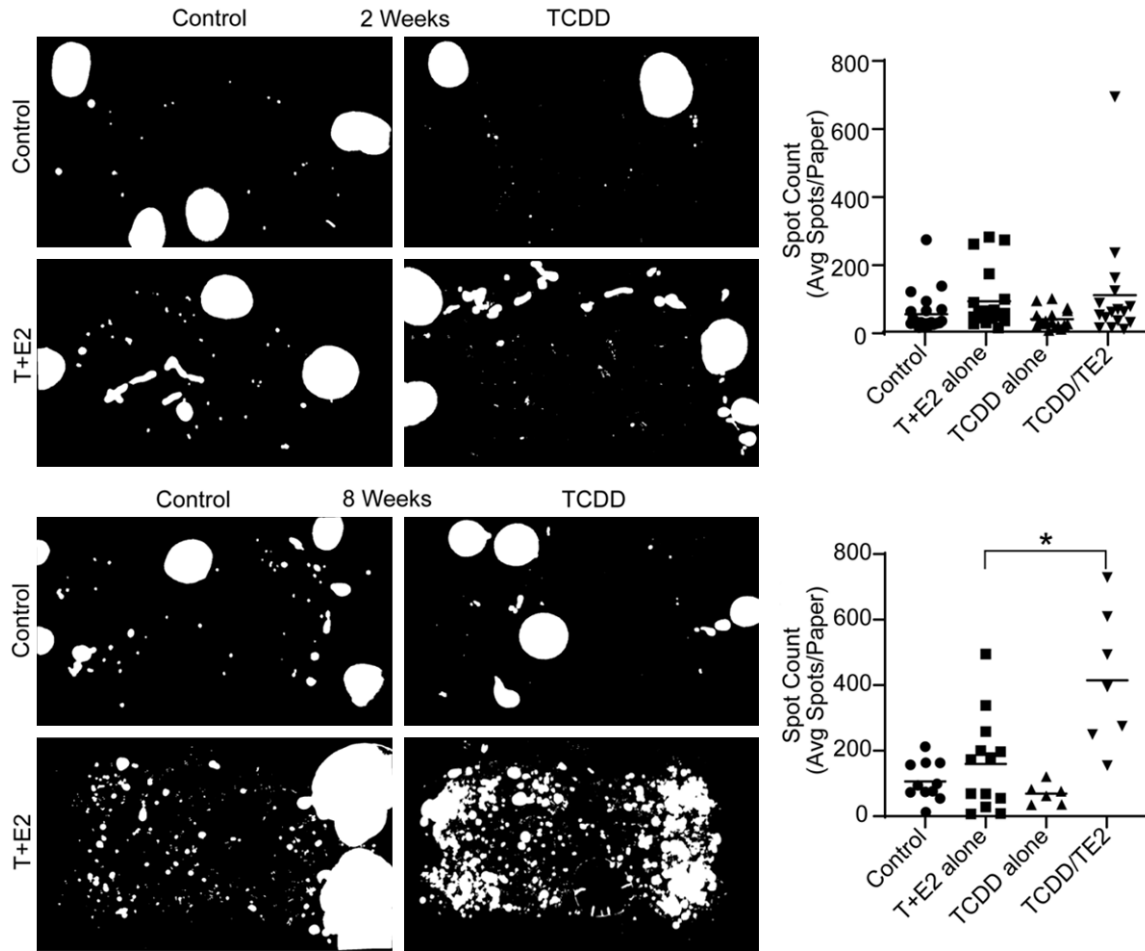


Figure 3. *In utero* and lactational TCDD exposure exacerbates voiding dysfunction in T+E2-treated wild type mice. Mice were treated as described in **Figure 1** and voiding function was measured by the void spot assay two and eight weeks post-implantation surgery. A representative void spot assay image is inset above each group (urine spots in white). Control mice and mice exposed to TCDD alone did not differ significantly in urinary spot count at two or eight weeks. TCDD/T+E2 mice did not differ in spot count at two weeks but had significantly more urine spots compared to T+E2 alone at eight weeks. Results are mean \pm SE, $n = 7$ to 19. Differences between groups were evaluated by Student's *t*-test. An asterisk identifies a difference between the TCDD/T+E2 group and T+E2 alone group, $P = 0.0343$.

rehydrated, and stained with antibodies against ryanodine receptor 1 (RYR1) (Abcam: ab2827, RRID: AB_2183052, 1:100, [22]). RYR1 was identified by proteomic analysis as the protein with the largest increase in abundance between TCDD/T+E2 and T+E2 alone groups. Tissues were co-stained with antibodies against E-Cadherin (CDH1) to visualize prostatic and urethral epithelium as histological landmarks (Cell signaling: 3195S, RRID: AB_2291471, 1:200, [23-25]). All fluorescent images used the following secondary antibodies: rhodamine red (Jackson ImmunoResearch: 711-295-152, RRID: AB_2340613, 1:250) and Alexa 647 (Jackson ImmunoResearch: 715-605-150, RRID: AB_2340862, 1:250).

Fluorophores were detected using 546 nm and 633 nm lasers and imaged using a SP8 confocal microscope (Leica, Wetzlar, Germany) fitted with a 20x oil-immersion objective (HC PL Apo CS2 NA = 0.75; Leica, Wetzlar, Germany). Intensity levels across the entire image were adjusted using Adobe Photoshop (version 20.0). Immunofluorescent pixels were quantified using the Max Entropy thresholding feature of ImageJ (Version 1.52e11) to determine the percent of immunostained pixels within the optical field (**Figure 7**).

Whole lower urinary tracts from five male TCDD/T+E2 mice and six T+E2 alone mice were collected eight weeks after T+E2 implantation

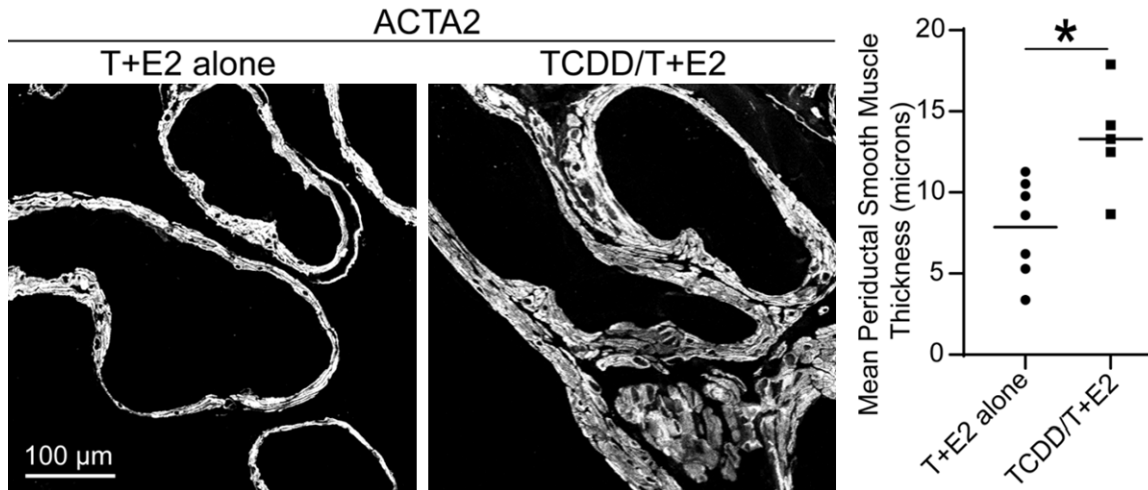


Figure 4. TCDD/T+E2 thickens dorsal prostate smooth muscle compared to T+E2 alone in C57Bl6/J mice. Dorsal prostate sections from mice treated with T+E2 alone or TCDD/T+E2 for eight weeks were stained with an antibody recognizing smooth muscle. Representative images of smooth muscle staining (white) are on the left. TCDD/T+E2 mice had significantly thicker smooth muscle in the proximal dorsal prostate of TCDD exposed mice (Student's *t*-test, mean \pm SEM, $\alpha = 0.05$, $P = 0.0137$, $n = 5$ to 7). Scale bar represents 100 μm .

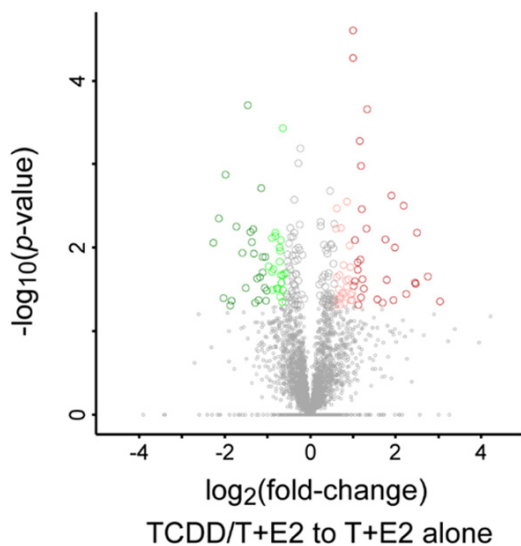


Figure 5. Prostate proteomic differences between TCDD/T+E2 and T+E2 alone mice. Volcano plot shows that 102 of 3641 identified proteins differ significantly in abundance ($P < 0.05$, Student's *t*-test; fold-change $\geq 50\%$) between TCDD/T+E2 and T+E2 alone groups. Results are representative of seven TCDD/T+E2 mice and six T+E2 mice. Light colored shapes indicate proteins with abundance differences of 50-100% between groups and dark colored shapes indicate peptides with abundance differences of $>100\%$.

for prostatic smooth muscle immunostaining. The dorsal prostate was imaged in representative regions. Tissues were stained with antibodies against actin alpha 2 (ACTA2) (Invitrogen:

PA5-18292, RRID: AB_10980764, 1:100, [26] and (ACTA2) (Leica: ncl-I-sma, RRID: AB_442-134, 1:200, [27]). Primaries were recognized with the following secondary antibodies: Rhodamine red (Jackson ImmunoResearch: 705-295-147, RRID: AB_2340423, 1:250), Rhodamine red (Jackson ImmunoResearch: 715-295-151, RRID: AB_2340832, 1:250). Smooth muscle thickness was determined as described previously [12], from two nonadjacent tissue sections per mouse using an optical micrometer in ImageJ (Version 1.52e11). Twenty measurements were made in a 20x field and averaged for each mouse and treatment group (Figure 4).

Data processing and statistical analysis

Differences in void spot assay outcomes, prostatic smooth muscle thickness, and immunofluorescent pixel density were evaluated using Student's *t*-test to identify significant differences ($P < 0.05$) between groups. Protein identification and relative quantification for prostate samples were achieved using MaxQuant software (v1.6.2.10; Max Planck Institute, Martinsried, Germany) [28], with protein- and peptide-level false discovery rate at 0.01, match between runs, intensity-based absolute quantification, and the Swiss-Prot *Mus musculus* database (v2019_05). Significant changes in prostate tissue proteomics were determined via volcano plot using Student's *t*-test and a

Developmental dioxin impacts adult urinary function

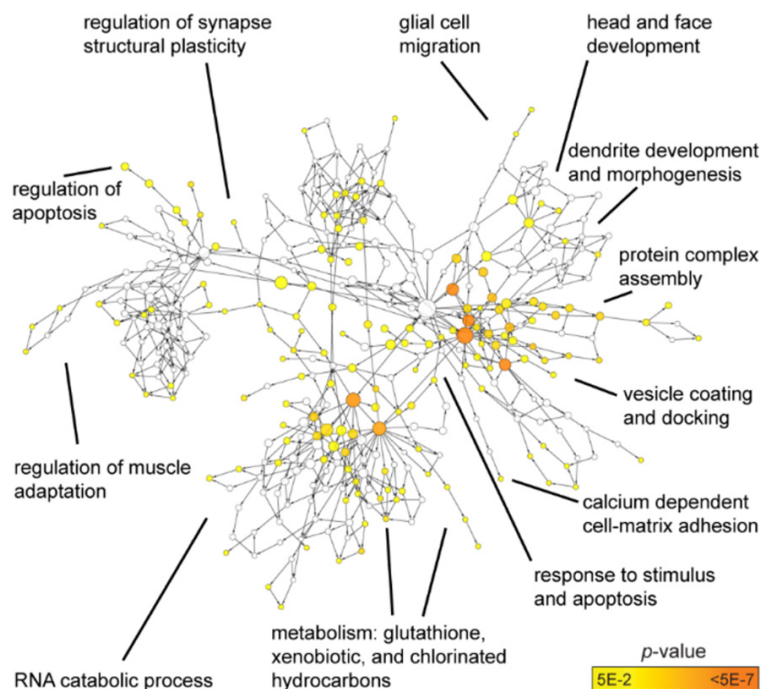


Figure 6. Significantly overrepresented biological processes among prostatic proteins that were more abundant in TCDD/T+E2 than T+E2 alone mice, as determined by gene ontology software (Cytoscape BiNGO tool, Hypergeometric test with B&H FDR correction; $n = 6$ to 7). Node size increases with increasing connectivity and color darkens with decreasing p -value.

permutation-based FDR ($\alpha = 0.05$; Perseus v1.6.2.3; Max Planck Institute, Martinsried, Germany) [29]. Significantly overrepresented biological processes in the prostate proteomics dataset were determined using the Hypergeometric test with Benjamini & Hochberg FDR correction ($\alpha = 0.05$; BiNGO tool, Cytoscape v3.6.1) [30, 31].

Results

In utero and lactational TCDD exposure acts by a non-malignant mechanism to exacerbate voiding dysfunction in T+E2-treated mice

We previously demonstrated that TCDD worsens T+E2-induced voiding dysfunction in mice [12], but that study was conducted with a mouse strain genetically prone to prostate cancer. It was therefore unclear whether TCDD acts through a malignant or non-malignant mechanism to impair urinary voiding. IUL TCDD exposure has the capacity to accelerate prostate cancer in genetically prone mice [14], but IUL TCDD exposure is not sufficient to drive neoplasia in non-susceptible C57BL/6J control

mice [13]. Pregnant dams were exposed to TCDD ($1 \mu\text{g}/\text{kg}$ oral maternal dose at E13.5) or corn oil vehicle ($5 \text{ mL}/\text{kg}$) and male offspring were then given T+E2 implants or sham surgeries at six weeks of age. We evaluated prostate histology two weeks after implantation surgery to test for the presence of neoplasia. Coalescing regions of epithelial hyperplasia and metaplasia were noted with infrequent areas of nuclear atypia. However, there was no evidence of high grade or invasive prostate neoplasia noted in the examined sections (**Figure 2**). TCDD/T+E2-treated mice therefore appear to be free of prostate malignancy when histological and physiological assessments were conducted in this study.

Frequent urination and dribbling are hallmarks of urinary dysfunction in aging men [32] and arise in T+E2-treated male mice [8]. We therefore evaluated spontaneous voiding behavior to test whether TCDD/T+E2 exacerbates voiding dysfunction. Evaluations included control mice (not exposed to either TCDD or T+E2), mice exposed to TCDD alone, T+E2 alone and TCDD/T+E2. Voiding behavior was evaluated two weeks after implantation surgery. There are no significant differences in urine spot count between TCDD alone and unexposed control mice (**Figure 3**). T+E2 alone significantly increased urine spot counts two weeks post-implantation surgery and there was no further increase by TCDD/T+E2 at this time (**Figure 3**). Voiding behaviors were evaluated again at eight weeks post-implantation surgery because obstructive voiding dysfunction is often progressive in mice and men. There were more urine spots at eight weeks post T+E2 in both groups compared to than two weeks, indicating urinary dysfunction had progressed. TCDD/T+E2 treatment resulted in a greater number of urine spots compared to mice treated with T+E2 alone at eight weeks post-implantation surgery (**Figure 3**). We conclude that voiding function in

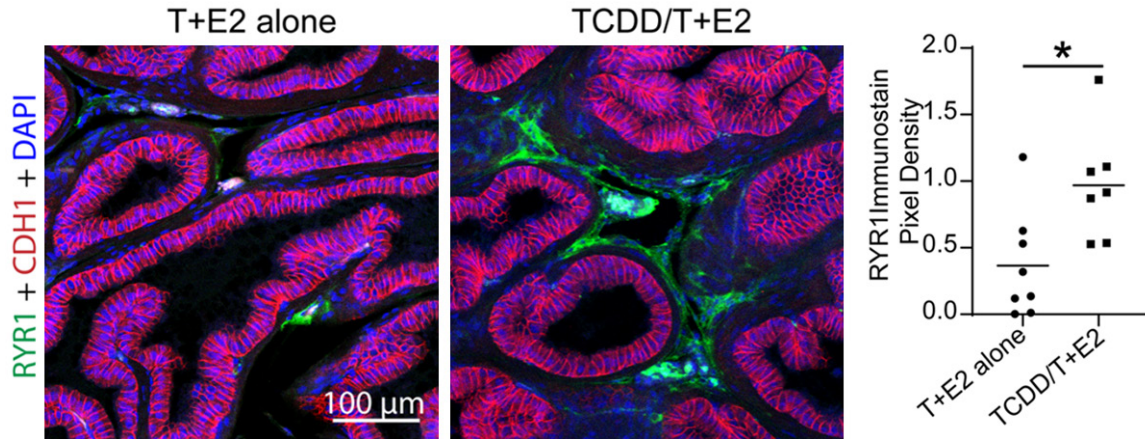


Figure 7. Ryanodine receptor (RYR1) immunostaining is more abundant in TCDD/T+E2 than T+E2 alone mice. Prostate tissue sections (10 µm) treated with TCDD/T+E2 or T+E2 alone were stained for ryanodine receptor 1 (RYR1) (green), CDH1 for epithelial cells (red), and DAPI for nuclei (blue). Quantification was performed on all prostate lobes and representative images in the dorsal prostate are shown above. The staining for RYR1 was significantly increased in TCDD/T+E2-treated prostate lobes compared to T+E2 alone (Student's *t*-test, $\alpha = 0.05$, $P = 0.014$; $n = 3$; mean \pm SEM; line represents mean of data). Scale bar is 100 µm.

the T+E2 alone group progressively worsens between two and eight weeks post-implantation surgery and that TCDD/T+E2 exacerbates this response through a non-malignant mechanism.

TCDD/T+E2 mice have thicker prostatic periductal smooth muscle than T+E2 alone mice

Prostatic smooth muscle dysfunction is one potential cause of urinary voiding dysfunction [6]. We previously demonstrated in a prostate cancer-prone mouse strain that prostatic smooth muscle was thicker in TCDD/T+E2 than T+E2 alone mice [12]. Others have reported increased peri-prostatic stroma thickness in rhesus macaques exposed *in utero* and via lactation to TCDD [33]. We conducted alpha smooth muscle actin immunostaining on prostate sections of wild type C57BL/6J mice (not genetically susceptible to prostate cancer) and found that prostatic periductal smooth muscle is thicker in TCDD/T+E2 mice (average of 15 microns) than T+E2 alone mice (average of seven microns) (**Figure 4**). We conclude that TCDD/T+E2 drives prostatic smooth muscle hypertrophy in mice that are not genetically prone to prostate cancer.

In utero and lactational TCDD exposure changes the abundance of a different set of proteins compared to those changed by T+E2 alone

We used a proteomic approach to refine the possible mechanisms by which TCDD/T+E2

exposure exacerbates voiding dysfunction. One possibility is that TCDD/T+E2 exposure acts by the same mechanism as T+E2 alone to impair voiding function. In such a scenario, we would expect that TCDD/T+E2 would act upon the same proteins and further increase the magnitude of abundance changes elicited by T+E2 alone. We previously identified a T+E2 prostatic protein signature (33 C57Bl/6J prostatic proteins significantly altered in abundance by T+E2 exposure, (Table S1; [16]). We tested whether TCDD/T+E2 significantly changed the abundance of these 33 proteins compared to T+E2 alone. All proteins from the signature except Glutathione S-transferase A2 (GSTA2) were successfully identified and quantified (Table S2). TCDD/T+E2 significantly altered the abundance of only one of the 33 signature proteins (Retinal dehydrogenase 2, ALDH1A2) compared to T+E2 alone, suggesting TCDD/T+E2 exacerbates voiding function through a different mode of action than T+E2 alone (Table S2).

In our global proteomics analysis, we identified 3641 mouse prostatic proteins by nanoLC-MS² (Table S3). Here we determined that TCDD/T+E2 significantly altered the abundance of 102 proteins compared to T+E2 alone (volcano plot: Student's *t*-test $\alpha = 0.05$, $\geq 50\%$ fold-change) (**Figure 5**). Biological processes significantly enriched among these 102 proteins included neural dysfunction, regulation of muscle and apoptosis, and metabolism of antioxi-

Developmental dioxin impacts adult urinary function

Table 1. Top 30 increased prostatic proteins in TCDD/T+E2 vs T+E2 alone ($n = 7$ vs $n = 6$, respectively)

Accession	Protein name	Protein Symbol	$-\log_{10}$ (p -value)	\log_2 (fold-change) TCDD/T+E2 to T+E2 alone
E9PZQ0	Ryanodine receptor 1	RYR1	1.35	3.04
Q921M4	Golgin subfamily A member 2	GOLGA2	1.65	2.74
O08539	Myc box-dependent-interacting protein 1	BIN1	2.18	2.49
Q8CHG3	GRIP and coiled-coil domain-containing protein 2	GCC2	1.56	2.46
P07744	Keratin, type II cytoskeletal 4	KRT4	1.58	2.45
P97443	Histone-lysine N-methyltransferase Smyd1	SMYD1	1.44	2.25
A2AAJ9	Obscurin	OBSCN	2.51	2.19
Q9R062	Glycogenin-1	GYG1	2.00	1.97
P33267	Cytochrome P450 2F2	CYP2F2	1.37	1.95
Q3V1D3	AMP deaminase 1	AMPD1	2.62	1.89
Q9CQ80	Vacuolar protein-sorting-associated protein 25	VPS25	1.62	1.79
Q8R3B1	1-phosphatidylinositol 4,5-bisphosphate phosphodiesterase delta-1	PLCD1	2.10	1.75
Q1XH17	Tripartite motif-containing protein 72	TRIM72	1.34	1.69
P04370	Myelin basic protein	MBP	1.38	1.57
P62322	U6 snRNA-associated Sm-like protein LSM5	LSM5	3.66	1.32
O09131	Glutathione S-transferase omega-1	GSTO1	2.23	1.31
O89001	Carboxypeptidase D	CPD	1.51	1.26
P04925	Major prion protein	PRNP	1.63	1.22
Q61206	Platelet-activating factor acetylhydrolase IB subunit beta	PAFAH1B2	2.46	1.20
Q9QZD8	Mitochondrial dicarboxylate carrier	SLC25A10	1.40	1.19
Q61301	Catenin alpha-2	CTNNA2	2.98	1.18
Q7TNV0	Protein DEK	DEK	1.86	1.18
P30115	Glutathione S-transferase A3	GSTA3	3.28	1.15
O55126	Protein NipSnap homolog 2	NIPSNAP2	1.31	1.13
Q9JKY5	Huntingtin-interacting protein 1-related protein	HIP1R	1.82	1.12
Q9D1H7	Golgi to ER traffic protein 4 homolog	GET4	1.73	1.11
Q62165	Dystroglycan	DAG1	1.59	1.05
Q8BHL8	Proteasome inhibitor PI31 subunit	PSMF1	2.09	1.04
P11087	Collagen alpha-1(I) chain	COL1A1	1.54	1.02
P36993	Protein phosphatase 1B	PPM1B	4.27	1.01

dants (**Figure 6**). Specifically, among the proteins most increased by TCDD/T+E2 compared to T+E2 alone are four with roles in muscle function: Ryanodine receptor 1 (RYR1), Obscurin (OBSCN), Tripartite motif-containing protein 72 (TRIM72), and Myc box-dependent-interacting protein 1 (BIN1). Others that increased have roles in neural function: Myelin basic protein (MBP), Catenin alpha-2 (CTNNA2), and Major prion protein (PRNP); fibrosis: Collagen alpha-1 (I) chain (COL1A1); oxidative stress defense: Glutathione S-transferase omega-1 (GSTO1), Glutathione S-transferase A3 (GSTA3); and drug metabolism: Cytochrome P450 2F2 (CYP2F2) (**Table 1**). Proteins that decreased in TCDD/T+E2 compared to T+E2 alone also have potential roles in urinary dys-

function, including the collagen crosslinker Procollagen-lysine, 2-oxoglutarate 5-dioxygenase 2 (PLOD2), the extracellular matrix component Laminin subunit beta-3 (LAMB3), the DNA repair protein BRISC and BRCA1-A complex member 2 (BABAM2), the nerve regulator Huntingtin-interacting protein 1 (HIP1), and the inflammation-related proteins Neutral cholesterol ester hydrolase 1 (NCEH1) and Ig gamma-2A chain C region secreted form (N/A) (**Table 2**). For a complete diagram of significantly enriched protein families see [Figure S1](#).

Immunohistochemistry was conducted to visualize the distribution of ryanodine receptor 1 protein, which was the protein that was most increased in abundance (among all proteins

Developmental dioxin impacts adult urinary function

Table 2. Top 30 decreased prostatic proteins in TCDD/T+E2 vs T+E2 alone ($n = 7$ vs $n = 6$, respectively)

Accession	Protein name	Protein Symbol	$-\log_{10}$ (p -value)	\log_2 (fold-change) TCDD/T+E2 to T+E2 alone
Q8CI04	Conserved oligomeric Golgi complex subunit 3	COG3	2.06	-2.26
A2RSQ1	Beta-galactosidase-1-like protein 3	GLB1L3	2.35	-2.14
Q9QXZ0	Microtubule-actin cross-linking factor 1	MACF1	1.40	-2.03
Q9R0B9	Procollagen-lysine,2-oxoglutarate 5-dioxygenase 2	PLOD2	2.88	-1.98
Q8BTY8	Sec1 family domain-containing protein 2	SCFD2	1.31	-1.87
Q91VA1	Choline transporter-like protein 4	SLC4Aa4	1.36	-1.85
P97494	Glutamate-cysteine ligase catalytic subunit	GCLC	2.25	-1.73
Q61087	Laminin subunit beta-3	LAMB3	1.94	-1.58
Q8K3W0	BRISC and BRCA1-A complex member 2	BABAM2	1.51	-1.51
Q9Z2Q6	Septin-5	SEPTIN5	3.70	-1.46
P01864	Ig gamma-2A chain C region secreted form	N/A	2.19	-1.40
Q61194	Phosphatidylinositol 4-phosphate 3-kinase C2	PIK3C2A	2.06	-1.37
Q8VD75	Huntingtin-interacting protein 1	HIP1	2.22	-1.34
Q62264	Thyroid hormone-inducible hepatic protein	THRSP	1.93	-1.32
P06281	Renin-1	REN1	1.34	-1.29
P35282	Ras-related protein Rab-21	RAB21	1.63	-1.24
P33622	Apolipoprotein C-III	APOC3	1.37	-1.21
Q9Z1G3	V-type proton ATPase subunit C 1	ATP6V1C1	1.64	-1.17
P01837	Immunoglobulin kappa constant	IGKC	2.72	-1.15
Q99K30	Epidermal growth factor receptor kinase substrate...	EPS8L2	1.70	-1.11
Q8VE62	Polyadenylate-binding protein-interacting protein 1	PAIP1	1.89	-1.11
Q00493	Carboxypeptidase E	CPE	1.52	-1.06
Q9CX30	Protein YIF1B	YIF1B	1.89	-1.05
Q02357	Ankyrin-1	ANK1	1.36	-1.03
Q8R0G9	Nuclear pore complex protein Nup133	NUP133	1.49	-1.01
Q69ZS7	HBS1-like protein	HBS1I	1.78	-0.96
Q8BLF1	Neutral cholesterol ester hydrolase 1	NCEH1	2.12	-0.89
Q8BK64	Activator of 90 kDa heat shock protein ATPase homolog 1	AHSA1	1.71	-0.89
PODOV1	Interferon-activable protein 205-B	MNDA	1.49	-0.88
P24547	Inosine 5'-monophosphate dehydrogenase 2	IMPDH2	1.74	-0.87

significantly increased) by TCDD/T+E2 compared to T+E2 alone. Ryanodine receptor 1 was distributed in the mouse prostatic stroma, where it encircled ducts and stained the area between ducts. Ryanodine receptor 1 immunostained pixel density was more abundant in TCDD/T+E2 dorsal prostate stroma compared to T+E2 alone, thereby validating an outcome of proteomics with an independent method (Figure 7).

Discussion

We found evidence that IUL TCDD exposure exacerbates urinary voiding dysfunction in

T+E2-treated wild type C57Bl6/J male mice. We show that T+E2 increases spontaneous urine spotting as early as two weeks and that the number of spots increase through at least eight weeks post-implantation surgery. Though TCDD/T+E2 and T+E2 alone groups did not significantly differ in urine spotting at two weeks, TCDD/T+E2 drove significantly more urine spotting at eight weeks compared to T+E2 alone (Figure 3). The pattern of urinary dysfunction (increased urine spots) is consistent with a progressive increase in voiding frequency, a bothersome symptom in men. The mechanism by which TCDD deteriorates voiding function in T+E2-treated mice has not been

Developmental dioxin impacts adult urinary function

resolved. Prostate cancer in men and mice has been linked to urinary dysfunction phenotypes [15]. As a result, our previous findings that TCDD/T+E2 exacerbated urinary dysfunction compared to T+E2 alone could not discriminate between a TCDD-driven progression of prostate malignancy and a separate action on benign urinary function. Here, we refine the potential mechanisms by demonstrating TCDD acts independent of tumorigenesis (**Figure 2**).

We show that TCDD/T+E2 thickens dorsal prostate smooth muscle compared to T+E2 alone, validating our previous finding in mice predisposed to neoplasia (**Figure 4**) [12]. This TCDD action on prostate anatomy has been observed in other tissues, specifically that TCDD hypertrophies penile smooth muscle [34]. Thickened prostate smooth muscle may indicate the muscle is contracting more frequently or with a greater intensity. Prostate smooth muscle thickening could be relevant because many men with urinary dysfunction are treated with alpha-1 adrenergic antagonists, which relax prostate smooth. It is unknown why some men may experience hyperactive prostatic smooth muscle. In addition, proteomic analysis revealed dysregulated muscle and calcium flux proteins, indicating smooth muscle may be an important target to investigate as a mechanism for TCDD-mediated exacerbation of T+E2-induced urinary voiding dysfunction (**Figure 6**). Additional studies into the impact of TCDD/T+E2 on prostate smooth muscle contractility would be beneficial in determining whether environmental chemical exposure can contribute to hypercontracted prostate smooth muscle.

To identify whether TCDD/T+E2 has a mode of action that differs from T+E2 alone, the trajectory of prostatic protein abundance changes was captured by sampling at two weeks post-implantation surgery, while urinary dysfunction was developing. Our prior analysis of prostatic proteomic changes in mice treated with T+E2 alone led us to hypothesize that TCDD/T+E2 exacerbated urinary dysfunction by further changing the abundance of proteins affected by T+E2. However, just one of 33 proteins known to be altered by T+E2 was further altered by TCDD/T+E2, suggesting the mode of action of TCDD/T+E2 differs from that of T+E2 treatment alone. T+E2 modulated proteins related to the acute phase response and oxidative

stress defense whereas TCDD/T+E2 significantly modulated other proteins representing processes that are important in urinary dysfunction, including muscle and calcium flux, neurologic function, fibrosis, response to oxidative stress, and inflammation (**Figures 5, 6**). TCDD/T+E2 dysregulated prostatic proteins linked to neurologic function (**Table 1**). TCDD and other AHR agonists can be toxic to the peripheral nervous system [35]. TCDD disrupts neural control of golden hamster thermoregulation [36] and increases activity of axons controlling rat aortic smooth muscle tone [37]. Dysregulation of axon function within the prostate is a potential mechanism of TCDD-mediated exacerbation of urinary voiding dysfunction, as men with urinary dysfunction often have increased autonomic activity [38].

We discovered that TCDD/T+E2 increases fibrillar collagen (COL1A1) protein abundance and decreases collagen crosslinker (PLOD2) abundance in C57BL/6J mouse prostate. Collagen deposition and prostate rigidity have been linked to lower urinary tract symptom severity and treatment resistance [39, 40]. TCDD/T+E2 exposure has been shown to disrupt collagen distribution [12]. Additionally, a maternal TCDD dose given to rhesus macaques during pregnancy caused increased prostatic fibrosis in male offspring [33]. Disrupted collagen distribution could stiffen the prostate, impairing passage of urine through the prostatic urethra. Further studies linking environmental chemical exposure to prostatic fibrosis would be beneficial for deciphering whether TCDD/T+E2 is acting via this mechanism.

We show that antioxidant proteins and inflammation-related proteins were dysregulated in the TCDD/T+E2 group compared to T+E2 alone. TCDD is a known immunomodulator [41] and promotes inflammation in the mouse testes [42], and modulates superoxide in mice [37]. It has been shown that men with prostate inflammation have significantly exacerbated urinary dysfunction [43]. Further research investigating prostate inflammation after TCDD/T+E2 exposure would determine whether inflammation is involved in the mechanism by which TCDD exacerbates urinary dysfunction.

Conclusion

Human exposure to TCDD continues despite widespread regulatory action. Human urologi-

Developmental dioxin impacts adult urinary function

cal outcomes of TCDD exposure, particularly exposure occurring during fetal and neonatal periods, are unknown. We showed that *in utero* and lactational TCDD exposure predisposes C57Bl6/J mice to T+E2-induced urinary dysfunction and increases prostatic periductal smooth muscle thickness. Future efforts will test the capacity of antifibrotics and muscle relaxers to alleviate voiding dysfunction and examine the specific contributions of proteins affected by TCDD exposure on prostate and urinary function.

Data deposition

The mass spectrometry proteomics data have been deposited to the ProteomeXchange Consortium via the PRIDE partner repository [44] with the dataset identifier PXD014752.

Acknowledgements

This work was also supported by National Institutes of Health through grants T32-ES007015, P30 CA014520, P20 DK097826, NIH/NIDDK U54 DK104310, NIH R01 ES01332, NIH R01 DK071801, and NIH P41GM108538, NIH-NCRR S10RR029531.

Disclosure of conflict of interest

None.

Address correspondence to: Chad M Vezina, Molecular and Environmental Toxicology Center, University of Wisconsin-Madison, 1656 Linden Dr, Madison, WI 53706, USA. Tel: +608-890-3235; E-mail: chad.vezina@wisc.edu

References

- [1] Oelke M, Bachmann A, Descalzeaud A, Emberton M, Gravas S, Michel MC, N'dow J, Nordling J and de la Rosette JJ; European Association of Urology. EAU guidelines on the treatment and follow-up of non-neurogenic male lower urinary tract symptoms including benign prostatic obstruction. *Eur Urol* 2013; 64: 118-140.
- [2] Rosen R, Altwein J, Boyle P, Kirby RS, Lukacs B, Meuleman E, O'Leary MP, Puppò P, Robertson C and Giuliano F. Lower urinary tract symptoms and male sexual dysfunction: the multinational survey of the aging male (MSAM-7). *Eur Urol* 2003; 44: 637-49.
- [3] Saigal CS and Joyce G. Economic costs of benign prostatic hyperplasia in the private sector. *J Urol* 2005; 173: 1309-1313.
- [4] Mitropoulos D, Anastasiou I, Giannopoulou C, Nikolopoulos P, Alamanis C, Zervas A and Dimopoulos C. Symptomatic benign prostate hyperplasia: impact on partners' quality of life. *Eur Urol* 2002; 41: 240-244.
- [5] McVary KT, Rademaker A, Lloyd GL and Gann P. Autonomic nervous system overactivity in men with lower urinary tract symptoms secondary to benign prostatic hyperplasia. *J Urol* 2005; 174: 1327-1433.
- [6] Caine M, Raz S and Zeigler M. Adrenergic and cholinergic receptors in the human prostate, prostatic capsule and bladder neck. *Br J Urol* 1975; 47: 193-202.
- [7] Bjornerem A, Straume B, Midtby M, Fonnebo V, Sundsfjord J, Svartberg J, Acharya G, Oian P and Berntsen GK. Endogenous sex hormones in relation to age, sex, lifestyle factors, and chronic diseases in a general population: the Tromso study. *J Clin Endocrinol Metab* 2004; 89: 6039-6047.
- [8] Nicholson TM, Ricke EA, Marker PC, Miano JM, Mayer RD, Timms BG, vom Saal FS, Wood RW and Ricke WA. Testosterone and 17beta-estradiol induce glandular prostatic growth, bladder outlet obstruction, and voiding dysfunction in male mice. *Endocrinology* 2012; 153: 5556-5565.
- [9] Nicholson TM, Moses MA, Uchtman KS, Keil KP, Bjorling DE, Vezina CM, Wood RW and Ricke WA. Estrogen receptor-alpha is a key mediator and therapeutic target for bladder complications of benign prostatic hyperplasia. *J Urol* 2015; 193: 722-729.
- [10] Keil KP, Abler LL, Altmann HM, Wang Z, Wang P, Ricke WA, Bjorling DE and Vezina CM. Impact of a folic acid-enriched diet on urinary tract function in mice treated with testosterone and estradiol. *Am J Physiol Renal Physiol* 2015; 308: F1431-F1443.
- [11] Lepor H. Pathophysiology of lower urinary tract symptoms in the aging male population. *Rev Urol* 2005; 7 Suppl 7: S3-S11.
- [12] Ricke WA, Lee CW, Clapper TR, Schneider AJ, Moore RW, Keil KP, Abler LL, Wynder JL, Lopez Alvarado A, Beaubrun I, Vo J, Bauman TM, Ricke EA, Peterson RE and Vezina CM. In utero and lactational TCDD exposure increases susceptibility to lower urinary tract dysfunction in adulthood. *Toxicol Sci* 2016; 150: 429-440.
- [13] Fritz WA, Lin TM, Moore RW, Cooke PS and Peterson RE. In utero and lactational 2,3,7,8-tetrachlorodibenzo-p-dioxin exposure: effects on the prostate and its response to castration in senescent C57BL/6J mice. *Toxicol Sci* 2005; 86: 387-395.
- [14] Moore RW, Fritz WA, Schneider AJ, Lin TM, Branam AM, Safe S and Peterson RE. 2,3,7,8-tetrachlorodibenzo-p-dioxin has both pro-carcinogenic and anti-carcinogenic effects on

Developmental dioxin impacts adult urinary function

- neuroendocrine prostate carcinoma formation in TRAMP mice. *Toxicol Appl Pharmacol* 2016; 305: 242-249.
- [15] Clark JA, Inui TS, Silliman RA, Bokhour BG, Krasnow SH, Robinson RA, Spaulding M and Talcott JA. Patients' perceptions of quality of life after treatment for early prostate cancer. *J Clin Oncol* 2003; 21: 3777-3784.
- [16] Thomas S, Hao L, DeLaney K, McLean D, Steinke L, Marker P, Vezina C, Li L and Ricke W. Spatiotemporal proteomics reveals the molecular consequences of hormone treatment in a mouse model of lower urinary tract dysfunction. In Review 2019.
- [17] Gasiewicz TA, Geiger LE, Rucci G and Neal RA. Distribution, excretion, and metabolism of 2,3,7,8-tetrachlorodibenzo-p-dioxin in C57BL/6J, DBA/2J, and B6D2F1/J mice. *Drug Metab Dispos* 1983; 11: 397-403.
- [18] Wegner KA, Abler LL, Oakes SR, Mehta GS, Ritter KE, Hill WG, Zwaans BM, Lamb LE, Wang Z, Bjorling DE, Ricke WA, Macoska J, Marker PC, Southard-Smith EM, Eliceiri KW and Vezina CM. Void spot assay procedural optimization and software for rapid and objective quantification of rodent voiding function, including overlapping urine spots. *Am J Physiol Renal Physiol* 2018; 315: F1067-F1080.
- [19] Erde J, Loo RR and Loo JA. Enhanced FASP (eFASP) to increase proteome coverage and sample recovery for quantitative proteomic experiments. *J Proteome Res* 2014; 13: 1885-1895.
- [20] Abler LL, Keil KP, Mehta V, Joshi PS, Schmitz CT and Vezina CM. A high-resolution molecular atlas of the fetal mouse lower urogenital tract. *Dev Dyn* 2011; 240: 2364-2377.
- [21] Turco AE, Cadena MT, Zhang HL, Sandhu JK, Oakes SR, Chathurvedula T, Peterson RE, Keast JR and Vezina CM. A temporal and spatial map of axons in developing mouse prostate. *Histochem Cell Biol* 2019; 152: 35-45.
- [22] Basnayake K, Mazaud D, Bemelmans A, Rouach N, Korkotian E and Holcman D. Fast calcium transients in dendritic spines driven by extreme statistics. *PLoS Biol* 2019; 17: e2006202.
- [23] Vasilaki E, Kanaki Z, Stravopodis DJ and Klinakis A. Dll1 marks cells of origin of ras-induced cancer in mouse squamous epithelia. *Transl Oncol* 2018; 11: 1213-1219.
- [24] Drubay V, Skrypek N, Cordiez L, Vasseur R, Schulz C, Boukrout N, Duchene B, Coppin L, Van Seuninghen I and Jonckheere N. TGF-betaRII knock-down in pancreatic cancer cells promotes tumor growth and gemcitabine resistance. Importance of STAT3 phosphorylation on S727. *Cancers (Basel)* 2018; 10.
- [25] Lloyd-Lewis B, Davis FM, Harris OB, Hitchcock JR and Watson CJ. Neutral lineage tracing of proliferative embryonic and adult mammary stem/progenitor cells. *Development* 2018; 145.
- [26] Almquist BD, Castleberry SA, Sun JB, Lu AY and Hammond PT. Combination growth factor therapy via electrostatically assembled wound dressings improves diabetic ulcer healing in vivo. *Adv Healthc Mater* 2015; 4: 2090-2099.
- [27] Wegner KA, Cadena MT, Trevena R, Turco AE, Gottschalk A, Halberg RB, Guo J, McMahon JA, McMahon AP and Vezina CM. An immunohistochemical identification key for cell types in adult mouse prostatic and urethral tissue sections. *PLoS One* 2017; 12: e0188413.
- [28] Cox J and Mann M. MaxQuant enables high peptide identification rates, individualized p.p.b.-range mass accuracies and proteome-wide protein quantification. *Nat Biotechnol* 2008; 26: 1367-1372.
- [29] Tyanova S, Temu T, Sinitcyn P, Carlson A, Hein MY, Geiger T, Mann M and Cox J. The perseus computational platform for comprehensive analysis of (prote)omics data. *Nat Methods* 2016; 13: 731-740.
- [30] Shannon P, Markiel A, Ozier O, Baliga NS, Wang JT, Ramage D, Amin N, Schwikowski B and Ideker T. Cytoscape: a software environment for integrated models of biomolecular interaction networks. *Genome Res* 2003; 13: 2498-2504.
- [31] Maere S, Heymans K and Kuiper M. BiNGO: a cytoscape plugin to assess overrepresentation of gene ontology categories in biological networks. *Bioinformatics* 2005; 21: 3448-3449.
- [32] Reynard JM, Lim C, Peters TJ and Abrams P. The significance of terminal dribbling in men with lower urinary tract symptoms. *Br J Urol* 1996; 77: 705-710.
- [33] Arima A, Kato H, Ise R, Ooshima Y, Inoue A, Muneoka A, Kamimura S, Fukusato T, Kubota S, Sumida H and Yasuda M. In utero and lactational exposure to 2,3,7,8-tetrachlorodibenzo-p-dioxin (TCDD) induces disruption of glands of the prostate and fibrosis in rhesus monkeys. *Reprod Toxicol* 2010; 29: 317-322.
- [34] Moon DG, Lee KC, Kim YW, Park HS, Cho HY and Kim JJ. Effect of TCDD on corpus cavernosum histology and smooth muscle physiology. *Int J Impot Res* 2004; 16: 224-230.
- [35] Iida M, Kim EY, Murakami Y, Shima Y and Iwata H. Toxic effects of 2,3,7,8-tetrachlorodibenzo-p-dioxin on the peripheral nervous system of developing red seabream (*pagrus major*). *Aquat Toxicol* 2013; 128-129: 193-202.
- [36] Gordon CJ, Yang Y and Gray LE Jr. Autonomic and behavioral thermoregulation in golden

Developmental dioxin impacts adult urinary function

- hamsters exposed perinatally to dioxin. *Toxicol Appl Pharmacol* 1996; 137: 120-125.
- [37] Kopf PG, Huwe JK and Walker MK. Hypertension, cardiac hypertrophy, and impaired vascular relaxation induced by 2,3,7,8-tetrachlorodibenzo-p-dioxin are associated with increased superoxide. *Cardiovasc Toxicol* 2008; 8: 181-193.
- [38] White CW, Xie JH and Ventura S. Age-related changes in the innervation of the prostate gland: implications for prostate cancer initiation and progression. *Organogenesis* 2013; 9: 206-215.
- [39] Bauman TM, Nicholson TM, Ablner LL, Eliceiri KW, Huang W, Vezina CM and Rieke WA. Characterization of fibrillar collagens and extracellular matrix of glandular benign prostatic hyperplasia nodules. *PLoS One* 2014; 9: e109102.
- [40] Ma J, Gharaee-Kermani M, Kunju L, Hollingsworth JM, Adler J, Arruda EM and Macoska JA. Prostatic fibrosis is associated with lower urinary tract symptoms. *J Urol* 2012; 188: 1375-1381.
- [41] Stevens EA, Mezrich JD and Bradfield CA. The aryl hydrocarbon receptor: a perspective on potential roles in the immune system. *Immunology* 2009; 127: 299-311.
- [42] Jin M, Lou J, Yu H, Miao M, Wang G, Ai H, Huang Y, Han S, Han D and Yu G. Exposure to 2,3,7,8-tetrachlorodibenzo-p-dioxin promotes inflammation in mouse testes: the critical role of Klotho in Sertoli cells. *Toxicol Lett* 2018; 295: 134-143.
- [43] Cakir SS, Polat EC, Ozcan L, Besiroglu H, Otunctemur A and Ozbek E. The effect of prostatic inflammation on clinical outcomes in patients with benign prostatic hyperplasia. *Prostate Int* 2018; 6: 71-74.
- [44] Vizcaino JA, Cote RG, Csordas A, Dianes JA, Fabregat A, Foster JM, Griss J, Alpi E, Birim M, Contell J, O'Kelly G, Schoenegger A, Ovelheiro D, Perez-Riverol Y, Reisinger F, Rios D, Wang R and Hermjakob H. The PRoteomics IDentifications (PRIDE) database and associated tools: status in 2013. *Nucleic Acids Res* 2013; 41: D1063-1069.

Developmental dioxin impacts adult urinary function

Table S1. Instrument inclusion list for targeted proteomics method

Protein represented	Pepide sequence	Charge	m/z	Mass
sp O08677 KNG1_MOUSE	DIPVDSPELK	2	556.795329	1111.5761
	TDGSPTFYFSFK	2	625.290411	1248.56627
sp O08807 PRDX4_MOUSE	QITLNDLPVGR	2	613.348594	1224.68264
	GLFIIDDK	2	460.758018	919.501483
sp O70570 PIGR_MOUSE	VNPSYIGR	2	453.245609	904.476666
	SSVTFECDLGR	2	635.790252	1269.56595
sp P00920 CAH2_MOUSE	EPITVSSEQMSHFR	2	824.393404	1646.77226
	VLEALHSIK	2	505.305667	1008.59678
sp P01027 CO3_MOUSE	IFTVDNLLPVGK	2	715.406109	1428.79767
	VVIEDGVGDAVLTR	2	721.896106	1441.77766
sp P01898 HA10_MOUSE	GYLQYAYDGR	2	603.28292	1204.55129
	TWTAADVAIIIR	2	694.880259	1387.74596
sp P07724 ALBU_MOUSE	LVQEVTDFAK	2	575.311146	1148.60774
	APQVSTPTLVEAAR	2	720.396273	1438.77799
sp P07758 A1AT1_MOUSE	VINDFVEK	2	546.308406	1090.60226
	DQSPASHEIATNLGDFAILYR	2	1203.09023	2404.1659
sp P09036 ISK1_MOUSE	IEPVLIR	2	420.271096	838.527639
	EASCHDAVAGCPR	2	715.300992	1428.58743
sp P10605 CATB_MOUSE	EIMAEIYK	2	506.754618	1011.49468
	EQWSNCTIGQIR	2	794.880464	1587.74637
sp P10648 GSTA2_MOUSE	ISSLPNVK	2	429.258185	856.501818
	FIQSPEDLEK	2	603.306061	1204.59757
sp P21614 VTDB_MOUSE	FSSSTFEQVNLVK	2	807.41212	1612.80969
	VPTANLENVLAEDFTEILSR	2	1221.14975	2440.28496
sp P22437 PGH1_MOUSE	VPDYPGDDGSVLVR	2	744.870088	1487.72562
	LILIGETIK	2	500.326068	998.637583
sp P23953 EST1C_MOUSE	AISESGVINTNVGK	2	744.406837	1486.79912
	MNEETASLLLR	2	638.83192	1275.64929
sp P35700 PRDX1_MOUSE	ATAVMPDGQFK	2	582.789524	1163.56449
	LVQAFQFTDK	2	598.819138	1195.62372
sp P46412 GPX3_MOUSE	FLVGPDPGIVMR	2	658.855198	1315.69584
	QEPGENSEILPSLK	2	770.896303	1539.77805
sp P47791 GSHR_MOUSE	LNTIYQNNLTK	2	661.359159	1320.70376
	ALLTPVAIAAGR	2	576.858598	1151.70264
sp P57096 PSCA_MOUSE	AIGLVTISK	2	500.823692	999.632832
	GCSSQCEDDSENYLGGK	2	1006.38584	2010.75714
sp P70269 CATE_MOUSE	AQGQLSEFWR	2	611.304187	1220.59382
	QFYSVFDR	2	531.256174	1060.49779
sp P70699 LYAG_MOUSE	FSETAQQAMR	2	584.774405	1167.53426
	EGYIPLQGPSLTTTESR	2	981.512562	1961.01057
sp P97449 AMPN_MOUSE	VMAVDALASSHPLSPADEIK	3	718.696421	2153.06743
	VVATTQMQAADAR	2	689.343183	1376.67181
sp Q00898 A1AT5_MOUSE	IFNSGADLSGITEENAPLK	2	988.502194	1974.98984
	LAQIHIPR	2	474.292894	946.571235
sp Q60928 GGT1_MOUSE	LFQPSIQLAR	2	586.842948	1171.67134
	FVDVSQVIR	2	531.800749	1061.58694
sp Q62148 AL1A2_MOUSE	LIQEAAGR	2	429.245609	856.476666

Developmental dioxin impacts adult urinary function

	IVGSPFDPTTEQGPQIDKK	2	1029.03112	2056.04769
sp Q8BND5 QSOX1_MOUSE	VPVLVESR	2	449.77146	897.528367
	VLNTESDLVNK	2	694.380623	1386.74669
sp Q8CFG8 CS1B_MOUSE	VPVTSLETCK	2	567.297181	1132.57981
	NSDPSPMYAGITALR	2	748.364115	1494.71368
sp Q8CFG9 C1RB_MOUSE	VIIHPDYR	2	506.782359	1011.55016
	VLNYVDWIK	2	575.318774	1148.623
sp Q8CIF4 BTD_MOUSE	ILSGDPYCEK	2	591.278989	1180.54342
	WNPCLEPFR	2	609.789858	1217.56516
sp Q8VCT4 CES1D_MOUSE	APEEILAEK	2	500.27149	998.528426
	FAPPQPAEPWSFVK	2	800.911559	1599.80856
sp Q91XE4 ACY3_MOUSE	NLGSVDFPR	2	502.761623	1003.50869
	VTVPALLR	2	434.78437	867.554188
sp Q99LJ1 FUCO_MOUSE	DLVGELGAAVR	2	550.308938	1098.60332
	DGLIVPIFQER	2	643.858795	1285.70304
sp Q9D154 ILEUA_MOUSE	FMTEDTTDAPFR	2	715.816467	1429.61838
	LGVQDLFSSSK	2	590.814053	1179.61355
sp Q9Z110 P5CS_MOUSE	GPVGLEGLLTK	2	592.847896	1183.68124
	GDECGLALGR	2	524.248023	1046.48149

Table S2. Results of targeted proteomics analysis

Inclusion	List Proteins	Identified	<i>p</i> -val <0.05 and fold-change ≥50%	Log ₂ (fold-change)
O08677	KNG1_MOUSE	Y	N	-0.32
O08807	PRDX4_MOUSE	Y	N	-0.29
O70570	PIGR_MOUSE	Y	N	-0.26
P00920	CAH2_MOUSE	Y	N	-0.37
P01027	CO3_MOUSE	Y	N	0.07
P01898	HA10_MOUSE	Y	N	-0.07
P07724	ALBU_MOUSE	Y	N	-0.13
P07758	A1AT1_MOUSE	Y	N	-0.14
P09036	ISK1_MOUSE	Y	N	-0.40
P10605	CATB_MOUSE	Y	N	-0.15
P10648	GSTA2_MOUSE	N	N/A	N/A
P21614	VTDB_MOUSE	Y	N	-0.31
P22437	PGH1_MOUSE	Y	N	0.12
P23953	EST1C_MOUSE	Y	N	-0.15
P35700	PRDX1_MOUSE	Y	N	-0.15
P46412	GPX3_MOUSE	Y	N	-0.14
P47791	GSHR_MOUSE	Y	N	-0.04
P57096	PSCA_MOUSE	Y	N	-0.11
P70269	CATE_MOUSE	Y	N	-1.13
P70699	LYAG_MOUSE	Y	N	-0.23
P97449	AMPN_MOUSE	Y	N	-0.52
Q00898	A1AT5_MOUSE	Y	N	0.44
Q60928	GGT1_MOUSE	Y	N	-0.42
Q62148	AL1A2_MOUSE	Y	Y	-0.06
Q8BND5	QSOX1	Y	N	-0.12
Q8CFG8	CS1B	Y	N	-1.24
Q8CFG9	C1RB	Y	N	-0.86

Developmental dioxin impacts adult urinary function

Q8CIF4	BTD	Y	N	0.00
Q8VCT4	CES1D	Y	N	0.10
Q91XE4	ACY3	Y	N	2.06
Q99LJ1	FUCO	Y	N	0.90
Q9D154	ILEUA	Y	N	0.08
Q9Z110	P5CS	Y	N	-0.14

Protenins with significant changes due to TCDD/T+E2 vs T+E2 alonev are indicated in green (Studen's t-test p -value <0.05 and \geq 50% fold-change).

Developmental dioxin impacts adult urinary function

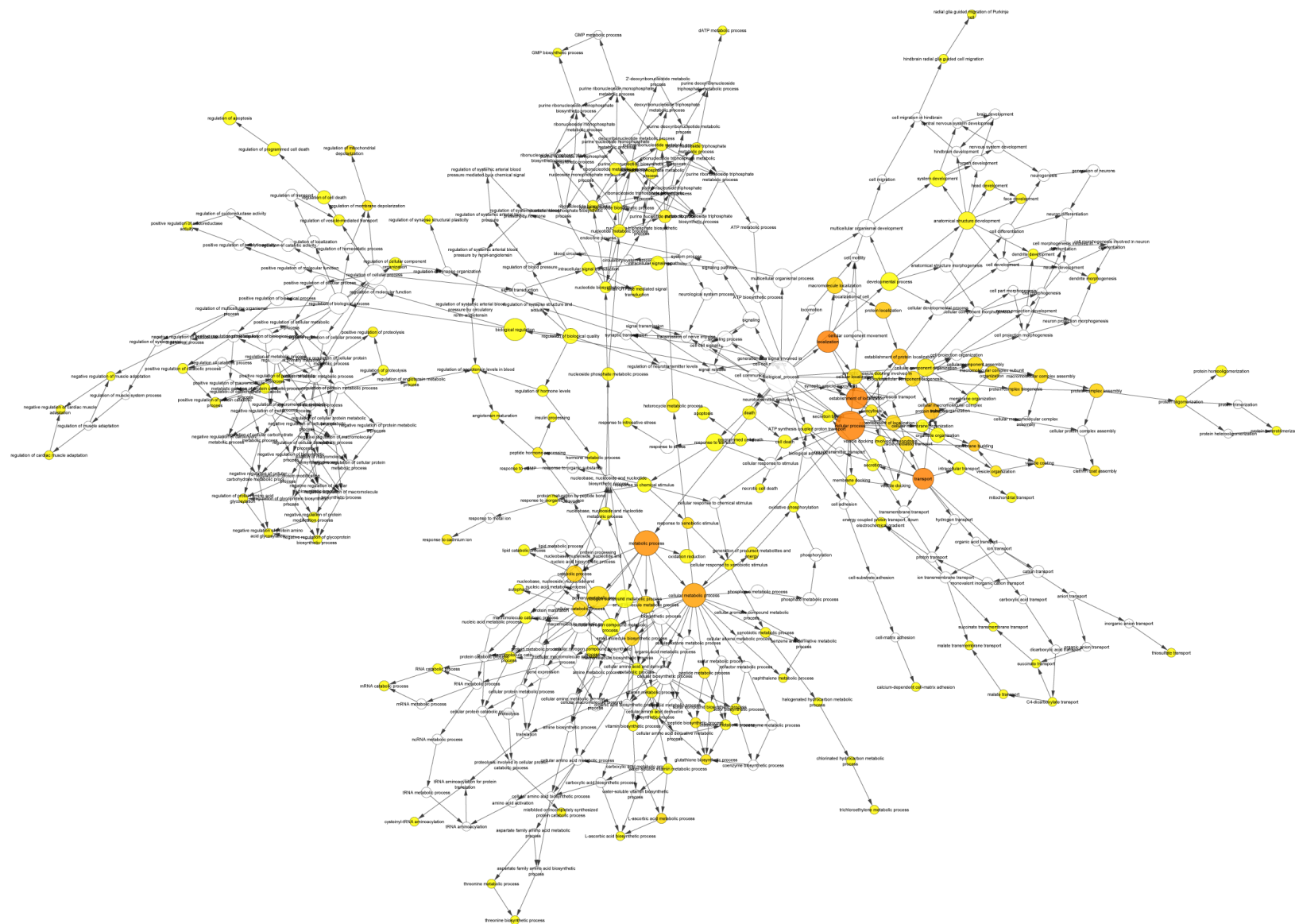


Figure S1. Cytoscape gene ontology: significantly enriched biological process with all labels.